Aptamer-Based Silver Nanoparticles Used for Intracellular Protein Imaging and Single Nanoparticle Spectral Analysis

Li Qiang Chen, Sai Jin Xiao, Li Peng, Tong Wu, Jian Ling, Yuan Fang Li, and Cheng Zhi Huang*

Education Ministry Key Laboratory on Luminescence and Real-Time Analysis, Southwest University, Chongqing 400715, P. R. China

Received: November 2, 2009; Revised Manuscript Received: January 9, 2010

Aptamer-adapted silver nanoparticles (Apt-AgNPs) were developed as a novel optical probe for simultaneous intracellular protein imaging and single nanoparticle spectral analysis, wherein AgNPs act as an illuminophore and the aptamer as a biomolecule specific recognition unit, respectively. It was found that streptavidin-conjugated and aptamer-functionalized AgNPs show satisfactory biocompatibility and stability in cell culture medium, and thus not only can act as a high contrast imaging agent for both dark-field light scattering microscope and TEM imaging but also can inspire supersensitive single nanoparticle spectra for potential intercellular microenvironment analysis. Further investigations showed that caveolae-related endocytosis is likely a necessary pathway for Apt-AgNPs labeled PrP^c internalization in human bone marrow neuroblastoma cells (SK-N-SH cells). The integrated capability of Apt-AgNPs to be used as light scattering and TEM imaging agents, along with their potential use for single nanoparticle spectral analysis, makes them a great promise for future biomedical imaging and disease diagnosis.

1. Introduction

Unique physical and chemical properties of metal nanostructures suggest a great deal of potential applications for biomedical imaging,[1–7] cancer clinical diagnosis, and therapy.[8–10] Among noble-metal nanoparticles, silver nanoparticles (AgNPs) exhibit salient features such as unique optical properties of localized surface plasmon resonance (LSPR) and super strong light scattering at their plasmon resonance frequency without any photobleaching.[11,12] Although these excellent optical features of AgNPs have been applied in single-particle sensing and *in vivo* imaging,[1,6,13,14] the biocompatibility and stability of Ag nanoprobes are still not satisfactory and await further improvement urgently. Furthermore, current applications of Ag nanoprobes are mostly based on antibodies, whose large molecular masses and high productive cost have, however, limited their further use.

As complements to antibody-based probes, a new generation of aptamer-based platform possesses many favorable characteristics such as cheapness, low molecular weight, easy preparation and modification. Aptamer, a certain sequence of DNA or RNA for a specific target to proteins, drugs, and metal irons, has been successfully used for protein detection,[15] cancer cell recognition and selective collection,[16] showing great potential in future biomedical applications. Thus, in this contribution, we prepared an aptamer-based AgNP (Apt-AgNP) probe with both stability and biocompatibility, wherein AgNPs were employed as illuminophores and aptamers as biomolecule-specific recognition agents, and demonstrated the applications of the modified probe for simultaneous intracellular protein imaging and single nanoparticle spectral analysis in cells.

Prion diseases, a family of rare progressive neurodegenerative disorders, impair the brain functions of human and other mammals seriously,[17] and the key mechanism of prion diseases is the conformational conversion of the cellular isoform of prion protein (PrP^c) to the insoluble pathogenic isoform (PrP^{Sc}).[18] Therefore, it is important to define the intracellular trafficking pathway of PrP^c for prevention and therapy of prion diseases. As a proof-of-concept experiments, we show how Apt-AgNP probes can be applied in intracellular PrP^c imaging and single nanoparticle spectral analysis in human bone marrow neuroblastoma cells (SK-N-SH cells).

2. Experimental Section

2.1. Reagents. The PrP^c aptamer sequence (5′-biotin-(C_6)-CTT ACG GTG GGG CAA TT-3′) in this contribution is the same as former reports,[19] synthesized by SBS Genetech Co., Ltd. (China), and used as received. Another ployT_{17} sequence (5′-biotin-(C_6)-TTT TTT TTT TTT TTT TT-3′) was used as a control. Streptavidin (SA) was purchased from Sigma-Aldrich (U.S.A.). Bovine serum albumin (BSA) was purchased from Shanghai Biology Products Institute (Shanghai, China). Other commercial reagents such as silver nitrate and trisodium citrate are analytical reagent grade without further purification. All water used is ultrapurified with an LD-50G-E Ultra-Pure Water System (Lidi Modern Waters Equipments Co., Chongqing, China).

2.2. Preparation and Characterization of Apt-AgNP Probes. Silver nanoparticles were prepared according to the modified Lee−Meisel method.[20] The size of AgNPs as prepared was measured with a Hitachi S-4800 scanning electron microscope (SEM) (Tokyo, Japan), and the concentration was calculated according to the extinction spectra of colloidal solution, wherein the extinction cross section of AgNPs ($c_{40nmAgNPs}$) was 8.0×10^{-11} cm^2 and the extinction coefficient ($\varepsilon_{40nmAgNPs}$) was 2.104×10^{10} $cm^{-1} \cdot M^{-1}$.[21] These AgNPs were functionalized with streptavidin according to the reported methods that modified gold nanoparticles with minor modifications.[22] Briefly, 80 μL of 1 $mg \cdot mL^{-1}$ streptavidin was added to the AgNP suspension (2 mL, 2.43 nM) of pH 6.7, which

* Corresponding author. Phone: +86-23-68254659. Fax: +86-23-68866796. E-mail: chengzhi@swu.edu.cn.

10.1021/jp9104618
Published on Web 01/29/2010

had been previously adjusted with 0.1 M K_2CO_3, and incubated using a rotary shaker at 37 °C for 120 min. The mixture was then centrifuged at 10 000 rpm for 15 min. After that, the sediment was washed and resuspended in PBS buffer solution to gain SA-AgNPs. Biotin-aptamer in PBS buffer was added into the SA-AgNP solution and incubated at 37 °C for 15 min. The final product (Apt-AgNPs) was acquired by centrifugation at 9000 rpm for 15 min. The pellet was resuspended and stored in PBS buffer solution containing 0.1% BSA. The extinction spectra and hydrodynamic diameter of the nanoparticle suspension were measured with an UV-3600 UV/vis/NIR spectrophotometer (Shimadzu, Japan) and an N5 Submicrometer Particle Size Analyzer (Beckman, USA), respectively.

2.3. SEM and TEM Imaging. The samples for SEM imaging were prepared by placing 20 μL of AgNP solution onto the aluminum substrate and allowed to dry at room temperature. Imaging was carried out under a Hitachi S-4800 SEM (Tokyo, Japan) at an accelerating voltage of 20 kV. For TEM imaging, cells were incubated with AgNP probes for 1 h at 37 °C with 5% CO_2 and then washed with PBS buffer three times, followed by fixation in 2.5% glutaraldehyde (0.2 M, phosphate buffer solution, pH 7.4) overnight at 4 °C. The cells were rinsed in PBS buffer, and postfixed in water, dehydrated through a graded ethanol series followed by acetone, and then washed two times in 100% propylene oxide. The propylene oxide was replaced with EPON 618 with a series of exchanges, 1:1, 1:2 propylene oxide: EPON 618, and finally incubated overnight with 100% EPON 618. The samples were placed in molds and polymerized in the oven at 60 °C for 24 h. After curing, the cells were cut out of the block, remounted, and sectioned. The ultrathin sections were picked up on copper grids, and selected samples were stained with 3% uranyl acetate. Afterward, samples were examined on a TECNAI10 transmission electron microscope (Philips, Holland).

2.4. Cell Culture and MTT Assay. Human bone marrow neuroblastoma (SK-N-SH) cells at a concentration of 20 000 cells·mL^{-1} were first plated on a 96-well tissue-culture cluster, and cultured at 37 °C with 5% CO_2 for 24 h to make cells adhere to the surface. The medium was then changed with 100 μL of fresh MEM (10% FBS) containing different amounts of bulk AgNPs and Apt-AgNP probes, respectively, and the cells were allowed to grow for another 20 h. After adding 100 μL of 3-(4,5-dimethylthiazol-2-yl)-2,5-diphenyl tetrazolium bromide (MTT) reagents at the concentration 5 mg·mL^{-1} into each well, the cells were allowed to grow for another 4 h until visible purple precipitate appeared. The medium was then removed and 100 μL of DMSO was added. The cluster vibrated for 10 min to liberate the crystals completely. Finally, the absorption at 490 nm was measured with a Molecular Devices Spectra-Max 190 Microplate Reader (California, USA).

2.5. Dark-Field Imaging and Single Nanoparticle Microspectra Characterization. In a typical experiment, a 1 mL suspension of SK-N-SH cells (about 10^5 cells·mL^{-1}) was plated onto a cover ship, grown for 2−3 days, then treated with 2.43 pM Apt-AgNPs (or the same concentration of PloyT-AgNPs for a control) for 1 h, rinsed with PBS buffer three times, fixed with 4% paraformaldehyde, and sealed with a small amount of glycerol. Dark-field imaging of AgNPs and cells was acquired with an Olympus BX-51 microscope (Tokyo, Japan), which was equipped with a highly numerical dark field condenser (U-DCW). The colorful dark-field light scattering photographs of AgNPs in cells were captured with an Olympus E-510 digital camera (Tokyo, Japan). The light scattering spectra of single particles in cells were carried out through the Olympus BX-51 dark-field system integrated with an Acton Research Micro-Spec 2300i monochromator and a Princeton Instruments PI-MAX intensified charge coupled device (ICCD) (Trenton, USA), as we reported previously.[23]

SCHEME 1: Schematic Illustration of Apt-AgNP Probes for Simultaneous Intracellular Protein Imaging and Single Nanoparticle Spectral Analysis

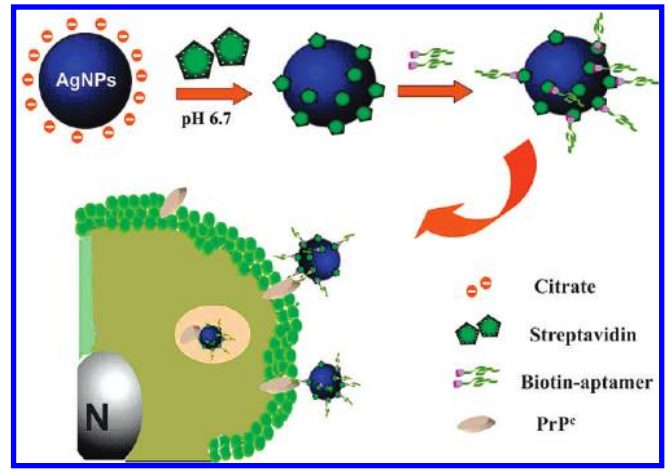

3. Results and Discussion

3.1. Synthesis and Characterization of Apt-AgNP Probes. Scheme 1 illustrates our basic idea by employing Apt-AgNP probes for imaging the intracellular endocytic pathways of prion protein in living cells. AgNPs are stable in solution owing to the electrostatic repulsion of the surface-adsorbed charged citrate layer.[24] The presence of an excess of noncharged or negative charged streptavidin can replace the citrate layer on the surface of AgNPs in neutral medium, and form AgNP-streptavidin conjugates (SA-Ag).[22] Then, biotin functionalized aptamers could be linked onto the surface of AgNPs through the high affinitive interaction between streptavidin and biotin, and thus, the Apt-AgNPs could be applied as biocompatible probes for imaging PrP^c in SK-N-SH cells. Therefore, our present contribution is composed of three parts, namely, the preparation of aptamer-functionalized AgNPs, the assessment of stability and biocompatibility of the prepared Apt-AgNPs probes, and the visual observation of the pathways of PrP^c labeled by Apt-AgNPs in neuroblast cells.

Monodispersed AgNPs with a size of 39.2 ± 12.4 nm (Figure 1a) were functionalized with streptavidin through physical electrostatic attraction. Photography shows that the Apt-AgNP solution is clear under visible light but scatters strong blue light under a common white LED light excitation (Figure 1b). The representative extinction spectra of AgNP, SA-AgNP, and Apt-AgNP suspensions are characterized at 444, 450, and 450 nm, respectively, illustrating that some red shift has occurred owing to the attachment of streptavidin onto the surface of AgNPs (Figure 1c). Dynamic light scattering (DLS) measurements revealed that the hydrodynamic diameters of AgNPs get increased from ∼40 to ∼60 nm (Figure 1d) with the modification of AgNPs, suggesting the modifications of streptavidin and aptamers on the surface of nanoparticles do not induce apparent aggregation in such a procedure.

Indeed, it is more challenging to functionalize stable AgNPs for biomedical application. We found that, during the process of functional modification, it is essential to adjust carefully the pH value of the medium, which is relative to the isoelectric point of proteins,[22] and to control the size of nanoparticles

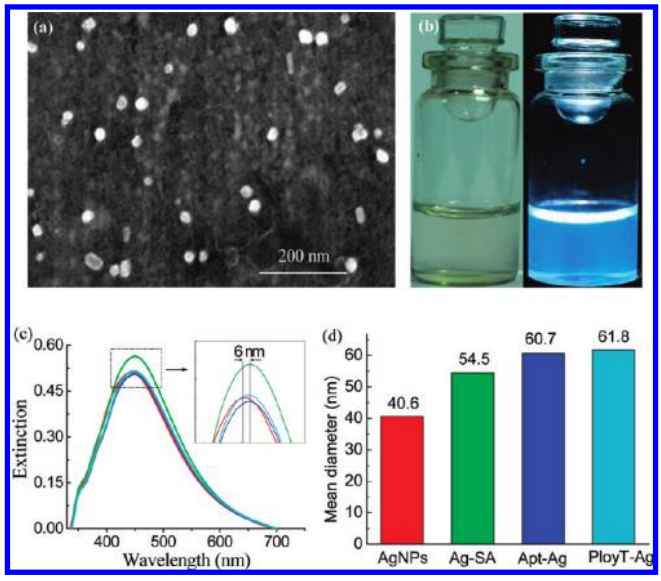

Figure 1. Features of aptamer-modifed AgNPs. (a) SEM image of AgNPs. (b) The visual photopictures of Apt-AgNP suspensions were taken under the excitation of visible light (left) and common white LED light (right), respectively. (c) Extinction spectra of AgNPs (red), AgNPs-SA (blue), Apt-AgNPs (green), and PloyT-AgNPs (cyan), respectively, with their corresponding characteristic absorption peaks at 444, 450, 450, and 450 nm. The inserted plot shows that a red shift of about 6 nm has occurred owing to the streptavidin attachment onto the surface of the nanoparticles. (d) Size information of bulk Ag, Ag-SA, Apt-AgNPs, and PloyT-AgNPs, as disclosed by dynamic light scattering (DLS) measurements.

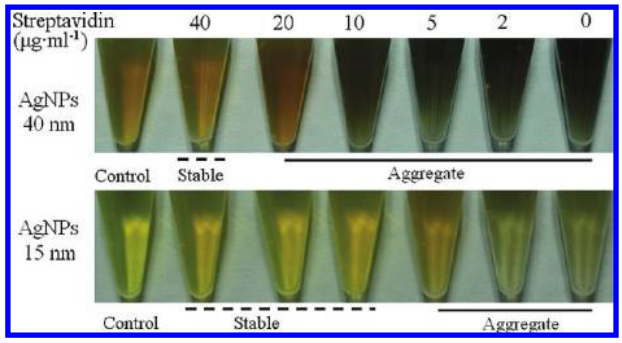

Figure 2. Streptavidin to prevent the aggregation of functional AgNPs with different sizes in salt solution. The pictures were taken after 30 min of incubation with the addition of NaCl into the medium, in which 30 min of incubation had been made for different concentrations of streptavidin with AgNP solution at pH 6.7. AgNP, 2.43 nM; NaCl, 0.1 M.

smaller than 50 nm. It was much easier to functionalize smaller AgNPs (~15 nm) than the bigger ones (~40 nm) with streptavidin to prevent the aggregation of the AgNPs in the salt solution (Figure 2). By the way, the optimal dose of streptavidin that we chose for functionalized ~40 nm AgNPs was 40 $\mu g \cdot mL^{-1}$.

3.2. Stability and Biocompatibility of Apt-AgNP Probes in Cell Culture Medium. In order to develop the Apt-AgNP probes for imaging of cells, their stability and biocompatibility should be considered at first. Figure 3a shows that the extinction at 450 nm of Apt-AgNP probes is stable in cell culture medium. MTT (3-(4,5-dimethylthiazol-2-yl)-2,5-diphenyltetrazolium bromide) assay revealed that the toxicity of Apt-AgNP probes to cells was mainly dependent on the dose of nanoparticles in the cell medium (Figure 3b). When the concentration of Apt-AgNPs was 2.43 pM, cell availability could reach ~90%, suggesting that a low dose of Apt-AgNP probes is very weakly toxic and

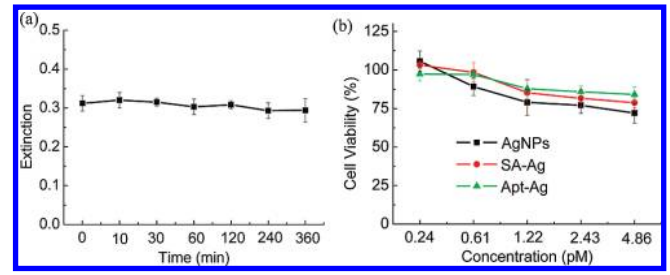

Figure 3. Stability and biocompatibility of Apt-AgNP probes. (a) The stability of Apt-AgNP probes in cell culture medium. Error bars were estimated from three replicate samples. (b) MTT assay demonstrating the minor toxicity to SK-N-SH cells of AgNPs, SA-AgNPs, and Apt-AgNPs after 24 h of incubation. Error bars were estimated from six replicate samples.

can be further used for live cell imaging. In addition, when the AgNP concentration increases from 0.61 to 4.86 pM, the cell availability of postmodification AgNPs (SA-AgNPs or Apt-AgNPs) was about ~5−10% higher than that of AgNPs without any modification, demonstrating that our modified procedure can improve the biocompatibility of AgNPs. A possible reason is that the binding of streptavidin to the surface of AgNPs inhibits the direct interaction between AgNPs and cells, improving the biocompatibility of Apt-AgNP probes owing to the introduction of streptavidin. In a word, all of these results illustrate that our Apt-AgNP probes have suitable properties for biomedical imaging under physiological conditions.

3.3. Simultaneous Intracellular Protein Imaging and Single Nanoparticle Spectral Analysis. With a dark-field microscope, we could clearly observe the distribution and light scattering properties of Apt-AgNP labels in living cells. Figure 4a,b shows the distribution and the LSPR light scattering properties of Apt-AgNPs probes in SK-N-SH cells. It is obvious that a lot of Apt-AgNP probes have bound to the neuroblast cells in the way of many bright color dots. Negative controls, which were made by incubating either $ployT_{17}$-AgNPs or AgNPs-SA with live cells under the same conditions, showed that there was no significant number of bound AgNPs in neuroblast cells (Figure 4c,d). Therefore, it is obvious that our Apt-AgNP probes could specifically target prion protein in living cells.

Figure 4e shows that the Apt-AgNPs in neuroblast cells were well individually dispersed in cytoplasm, and exhibited multicolors including blue, green, and orange, illustrating that the Apt-AgNPs could disclose some local environmental information, since light-scattering properties of metal nanoparticles are dependent on the composition, size, and shape of nanoparticles as well as their surrounding medium according to the Rayleigh and Mie theory.[25,26] The different shape of Apt-AgNPs is responsible for their multicolors, because a small quantity of Ag nanorods, which possess different light scattering colors comparing with the AgNPs,[23] could be observed in SEM images (Figure 1a). Furthermore, the different light scattering colors could also arise from different shapes, size of spheres, or aggregates of Apt-AgNPs in cells. In addition, the multicolor of Apt-AgNPs is also likely caused by the different local circumstances in each organelle, since the Apt-AgNPs were transported into a series of intracellular regions which have different acid internal environments. For example, late lysosome has proved to bring more acid internal environments compared with other intracellular organelles.

Combining a Micro-Spec monochromator with an intensified charge coupled device, we could simultaneously achieve the dark-field light scattering imaging and cellular single nanopar-

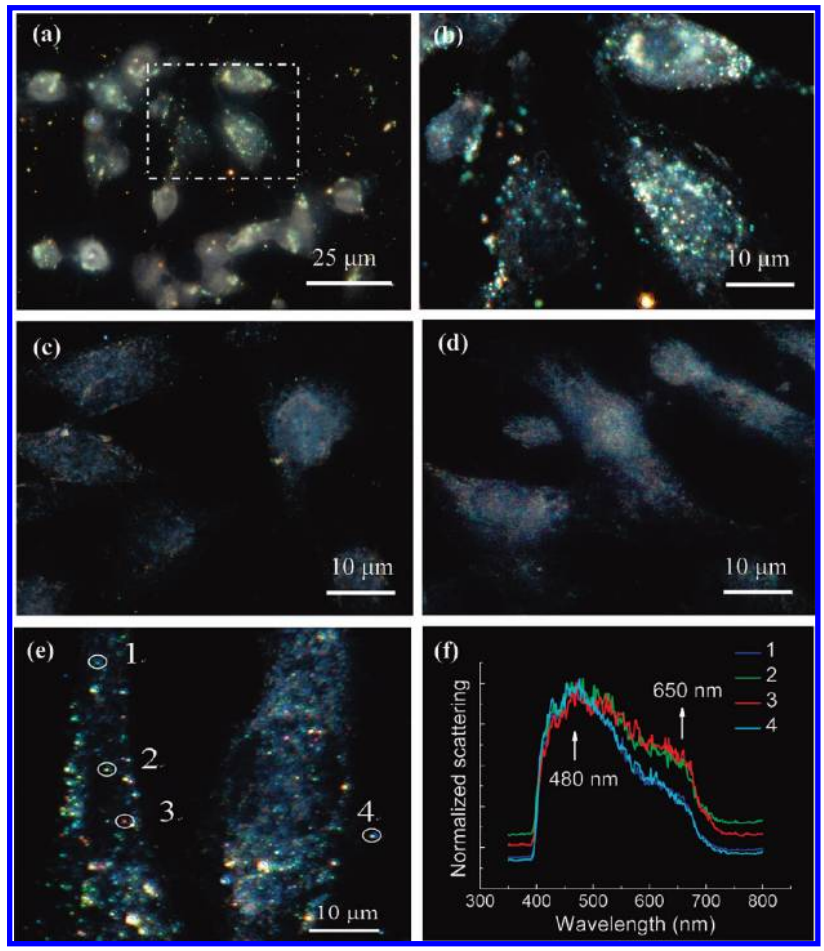

Figure 4. Dark-field light scattering images and single nanoparticle spectral analysis of PrP^c labeled with Apt-AgNPs in living cells. (a, b) Most of the cells were marked by Apt-AgNP probes. Image b is the local enlarged view of the corresponding square area in image a. (c, d) Control experiment, cell incubation with $PloyT_{17}$-AgNPs or AgNPs-SA, showing that few AgNPs could be found in cells. (e, f) Representative image of single Apt-AgNP labels and their corresponding single particle spectra in SK-N-SH cells.

ticle spectral analysis. The LSPR light scattering spectra of these Apt-AgNPs with the same color distributed either inside or outside of cells are quite similar (curves 1 and 4 in Figure 4e,f), but the ones scattering blue light (curve 1) are obviously different from that scattering green or orange light (curves 2 and 3). The blue ones (curve 1), characterized at about 480 nm, should be ascribed to the plasmon resonance scattering of the silver nanosphere,[23] while the green and orange ones, characterized two scattering at 480 and 650 nm, might be ascribed to different size and shape dependent LSPR properties of Apt-AgNP labels.[6,23,25,26] Such multicolor and superior sensitivity of light scattering spectra suggested the potential use of Apt-AgNPs as a nanosensor for single-particle sensing in living cells.

3.4. Internalized Pathway Investigation. PrP^c is a cell-surface glycosylphosphatidylinositol (GPI)-anchored protein that is constitutively internalized into cytoplasm.[27] In order to identify the intracellular pathways of PrP^c labeled by Apt-AgNPs in neuroblast cells, TEM was employed for further testing. As Figure 5a shows, AgNPs translocate across the membrane and get into the cytoplasm but could not arrive at the nuclear, indicating that AgNPs exhibit passive uptake through the PrP^c dependent pathway. We further observed that Apt-AgNPs are located in plasma membrane, endocytic structure, lysosome, and mitochondria (Figure 5a,b). These results are consistent with the previous reports that most PrP^c labeled with 5 nm gold nanoparticles were internalized *via* a caveolae-dependent endocytic pathway in Chinese hamster ovary cells.[28] It has reported that cell-surface PrP^c can transport into cytoplasm through three

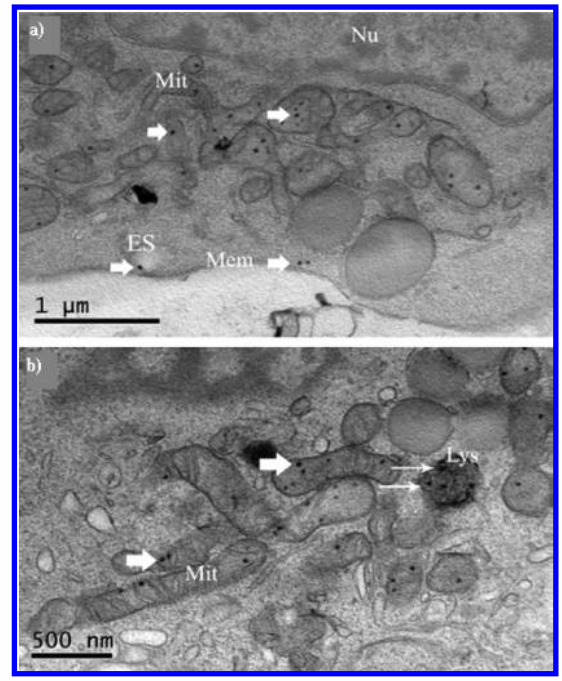

Figure 5. TEM images showing the PrP^c dependent Apt-AgNP probes uptake by SK-N-SH cells. (a) Apt-AgNP labels translocated across the plasma membrane and entry into the cytoplasm of neuroblast cells distributing in plasma membrane, endocytic structure. (b) Lysosome and mitochondria. ES, endocytic structure; Lys, lysosome; Mem, membrane; Mit, mitochondria; Nu, nuclear.

endocytic pathways, including calthrin-mediated endocytosis, caveolin-related endocytosis, as well as nonclathrin and non-caveolin but raft-dependent endocyosis.[29] Therefore, we conclude that the caveolae-related endocytosis is likely a necessary pathway for Apt-AgNP labeling PrP^c internalization in SK-N-SH cells.

Conclusion

In summary, we have developed a novel aptamer-based AgNP bioprobe for simultaneous intracellular protein imaging and single nanoparticle spectral analysis. Compared with other optical nanoprobes, Apt-AgNP probes possess two main advantages including ultrabright scattering light without any photobleaching and easy preparation with low product cost. With excellent stability and biocompatibility, Apt-AgNP probes cannot only act as a high contrast imaging agent for both dark-field light scattering microscopy and TEM imaging but also inspire supersensitive single nanoparticle spectra for potential intercellular microenvironment analysis. Our results also illustrate that the caveolae-related endocytosis is likely a necessary pathway for Apt-AgNP labeling PrP^c internalization in SK-N-SH cells.

Acknowledgment. All authors are grateful to the financial support from the Ministry of Science and Technology of the People's Republic of China (2006CB 933100) and the National Natural Sciences Foundation of China (20775061).

References and Notes

(1) Schultz, S.; Smith, D. R.; Mock, J. J.; Schultz, D. A. *Proc. Natl. Acad. Sci. U.S.A.* **2000**, *97* (3), 996–1001.
(2) Boyer, D.; Tamarat, P.; Maali, A.; Lounis, B.; Orrit, M. *Science* **2002**, *297* (5584), 1160–1163.
(3) Yu, C.; Nakshatri, H.; Irudayaraj, J. *Nano Lett.* **2007**, *7* (8), 2300–2306.
(4) Kumar, S.; Harrison, N.; Richards-Kortum, R.; Sokolov, K. *Nano Lett.* **2007**, *7* (5), 1338–1343.
(5) Choi, Y.; Kang, T.; Lee, L. P. *Nano Lett.* **2009**, *9* (1), 85–90.
(6) Huang, T.; Nallathamby, P. D.; Gillet, D.; Xu, X.-H. N. *Anal. Chem.* **2007**, *79*, 7708–7718.
(7) Hu, R.; Yong, K.-T.; Roy, I.; Ding, H.; He, S.; Prasad, P. N. *J. Phys. Chem. C* **2009**, *113*, 2676–2684.
(8) El-Sayed, I. H.; Huang, X.; El-Sayed, M. A. *Nano Lett.* **2005**, *5* (5), 829–834.
(9) Huang, X.; EI-Sayed, I. H.; Qian, W.; EI-Sayed, M. A. *J. Am. Chem. Soc.* **2006**, *128*, 2115–2120.
(10) Popovtzer, R.; Agrawal, A.; Kotov, N. A.; Popovtzer, A.; Balter, J.; Carey, T. E.; Kopelman, R. *Nano Lett.* **2008**, *8* (12), 4593–4596.
(11) Aslan, K.; Lakowicz, J. R.; Geddes, C. D. *Curr. Opin. Chem. Biol.* **2005**, *9* (5), 538–544.
(12) Jain, P. K.; Huang, X.; El-Sayed, I. H.; El-Sayed, M. A. *Acc. Chem. Res.* **2008**, *41* (12), 1578–1586.
(13) Lee, K. J.; Nallathamby, P. D.; Browning, L. M.; Osgood, C. J.; Xu, X.-H. N. *ACS Nano* **2007**, *1* (2), 133–143.
(14) Nallathamby, P. D.; Lee, K. J.; Xu, X.-H. N. *ACS Nano* **2008**, *2* (7), 1371–1380.
(15) Johnson, S.; Evans, D.; Laurenson, S.; Paul, D.; Davies, A. G.; Ko Ferrigno, P.; Wälti, C. *Anal. Chem.* **2008**, *80*, 978–983.
(16) Herr, J. K.; Smith, J. E.; Medley, C. D.; Shangguan, D.; Tan, W. *Anal. Chem.* **2006**, *78*, 2918–2924.
(17) Prusiner, S. B. *Proc. Natl. Acad. Sci. U.S.A.* **1998**, *95* (23), 13363–13383.
(18) Aguzzi, A.; Polymenidou, M. *Cell* **2004**, *116* (2), 313–327.
(19) Takemura, K.; Wang, P.; Vorberg, I.; Surewicz, W.; Priola, S. A.; Kanthasamy, A.; Pottathil, R.; Chen, S. G.; Sreevatsan, S. *Exp. Biol. Med.* **2006**, *231* (2), 204–214.
(20) Lee, P. C.; Meisel, D. *J. Phys. Chem.* **1982**, *86* (17), 3391–3395.
(21) Evanoff, D. D., Jr.; Chumanov, G. *J. Phys. Chem. B* **2004**, *108*, 13957–13962.
(22) Zhang, C.; Zhang, Z.; Yu, B.; Shi, J.; Zhang, X. *Anal. Chem.* **2002**, *74*, 96–99.
(23) Ling, J.; Li, Y. F.; Huang, C. Z. *Anal. Chem.* **2009**, *81* (4), 1707–1714.
(24) Li, X.; Zhang, J.; Xu, W.; Jia, H.; Wang, X.; Yang, B.; Zhao, B.; Li, B.; Ozaki, Y. *Langmuir* **2003**, *19*, 4285–4290.
(25) Yguerabide, J.; Yguerabide, E. E. *Anal. Biochem.* **1998**, *262* (2), 137–156.
(26) Yguerabide, J.; Yguerabide, E. E. *Anal. Biochem.* **1998**, *262* (2), 157–176.
(27) Prado, M. A. M.; Alves-Silva, J.; Magalhaes, A. C.; Prado, V. F.; Linden, R.; Martins, V. R.; Brentani, R. R. *J. Neurochem.* **2004**, *88* (4), 769–781.
(28) Peters, P. J.; Mironov, A., Jr.; Peretz, D.; van Donselaar, E.; Leclerc, E.; Erpel, S.; DeArmond, S. J.; Burton, D. R.; Williamson, R. A.; Vey, M.; Prusiner, S. B. *J. Cell Biol.* **2003**, *162* (4), 703–717.
(29) Campana, V.; Sarnataro, D.; Zurzolo, C. *Trends Cell Biol.* **2005**, *15* (2), 102–111.

JP9104618